

This is the accepted manuscript version of the contribution published as:

Vystavna, Y., Schmidt, S.I., Diadin, D., Rossi, P.M., Vergeles, Y., Erostate, M., Yermakovych, I., Yakovlev, V., **Knöller, K.**, Vadillo, I. (2019):
Multi-tracing of recharge seasonality and contamination in groundwater: A tool for urban water resource management
Water Res. **161** , 413 - 422

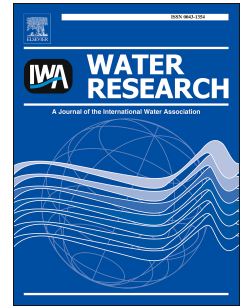
The publisher's version is available at:

<http://dx.doi.org/10.1016/j.watres.2019.06.028>

Accepted Manuscript

Multi-tracing of recharge seasonality and contamination in groundwater: A tool for urban water resource management

Y. Vystavna, S.I. Schmidt, D. Diadin, P.M. Rossi, Y. Vergeles, M. Erostate, I. Yermakovych, V. Yakovlev, K. Knöller, I. Vadillo



PII: S0043-1354(19)30539-1

DOI: <https://doi.org/10.1016/j.watres.2019.06.028>

Reference: WR 14784

To appear in: *Water Research*

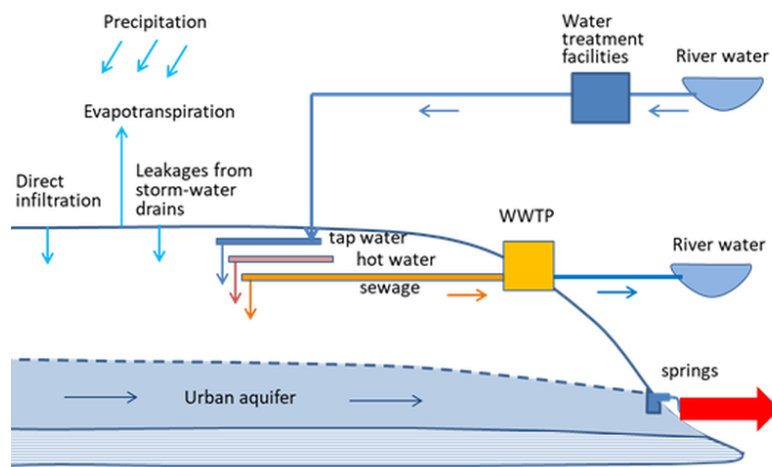
Received Date: 10 December 2018

Revised Date: 4 June 2019

Accepted Date: 11 June 2019

Please cite this article as: Vystavna, Y., Schmidt, S.I., Diadin, D., Rossi, P.M., Vergeles, Y., Erostate, M., Yermakovych, I., Yakovlev, V., Knöller, K., Vadillo, I., Multi-tracing of recharge seasonality and contamination in groundwater: A tool for urban water resource management, *Water Research* (2019), doi: <https://doi.org/10.1016/j.watres.2019.06.028>.

This is a PDF file of an unedited manuscript that has been accepted for publication. As a service to our customers we are providing this early version of the manuscript. The manuscript will undergo copyediting, typesetting, and review of the resulting proof before it is published in its final form. Please note that during the production process errors may be discovered which could affect the content, and all legal disclaimers that apply to the journal pertain.



Sewage inputs

Nitrate
Chloride
Illicit drugs
Pesticides

ACCEPTED MANUSCRIPT

1 **Multi-tracing of recharge seasonality and contamination in groundwater: a tool for**
2 **urban water resource management**

3 Vystavna Y.^{1,2}, Schmidt S.I.¹, Diadin D.², Rossi P.M.³, Vergeles Y.², Erostate M.^{4,5},

4 Yermakovych I.², Yakovlev V.^{2,6}, Knöller K.⁷, Vadillo I.⁸

5 ¹Institute of Hydrobiology, Biology Centre of the Academy of Sciences of the Czech
6 Republic, Na Sádkách 7, 37005, České Budějovice, the Czech Republic,
7 yuliya.vystavna@hbu.cas.cz

8 ²Department of Environmental Engineering and Management, O.M. Beketov National
9 University of Urban Economy in Kharkiv, vul. Marshala Bazhanova 17, 61002, Kharkiv,
10 Ukraine

11 ³Water, Energy and environmental Engineering Research Unit, University of Oulu, P.O. Box
12 4300, 90014, Oulu, Finland.

13 ⁴Université de Corse Pascal Paoli, Faculté des Sciences et Techniques, Laboratoire
14 d'Hydrogéologie, Campus Grimaldi, BP 52, F-20250, Corte, France

15 ⁵CNRS, UMR 6134, SPE, F-20250, Corte, France

16 ⁶Water Quality Laboratory "Playa", vul. Hanna 10, 61001, Kharkiv, Ukraine

17 ⁷Helmholtz Centre for Environmental Research – UFZ, Department of Catchment Hydrology,
18 Theodor-Lieser-Str. 4, 06120, Halle, Germany

19 ⁸Group of Hydrogeology, Faculty of Science, University of Malaga, 29071, Malaga, Spain.

20

21 **Abstract**

22 In this study, sources of recharge and contamination in urban groundwater and in
23 groundwater underneath a forest in the same aquifer were determined and compared. Data on
24 hydro-chemical parameters and stable isotopes of water were collected in urban and forest
25 springs in the Kharkiv region, Ukraine, over a period of 12 months. Groundwater transit time
26 and precipitation contribution were calculated using hydrogeological data and stable isotopes
27 of water to delineate groundwater recharge conditions. Hydro-chemical data, stable isotopes
28 and emerging contaminants were used to trace anthropogenic groundwater recharge and

29 approximate sewage and tap water contributions to the aquifer. The results indicated that each
30 spring had unique isotopic signatures that could be explained by recharge conditions,
31 groundwater residence time, and specific mixing patterns with sewage and water leaks.
32 Elevated nitrate content, stable isotopes of nitrate, and the presence of emerging pollutants
33 (mainly illicit drugs) in most of the urban springs confirmed mixing of urban groundwater
34 with sewage leaks. These leaks amounted to up to 25% of total recharge and exhibited
35 seasonal variations in some springs. Overall, the results show that urban groundwater receives
36 variable seasonal contributions of anthropogenic components that increase the risk to the
37 environment and human health, and reduce its usability for drinking water production. The
38 multi-tracing approach presented can be useful for other cities worldwide that have similar
39 problems of poor water management and inadequate sewage and water supply infrastructure.

40

41 **Keywords:** urban hydrology; stable isotopes; emerging compounds; aquifer; nitrate;
42 pesticide.

43

44 **1. Introduction**

45 Groundwater is an important source of drinking water worldwide and its role is
46 growing due to deterioration of surface water quality and quantity under the impact of climate
47 variability, contamination, and run-off re-allocation (FAO 2011, WWAP 2015). Surface water
48 and groundwater quality has been improved in the European Union (EU) (European
49 Commission 2012), mainly due to a number of water regulations (i.e., EU WFD 2000,
50 Groundwater Directive 2006). However, in many countries that share transboundary EU
51 surface water and aquifers, for example Ukraine, there is great concern regarding the low
52 quality and quantity of available groundwater resources because of ongoing and increasing

53 contamination (Yakovlev et al. 2015), and a lack of appropriate environmental regulations
54 (Vystavna et al. 2018a,b).

55 Drinking water supply from groundwater depends strongly on the seasonality of
56 recharge, climate, and contamination (Griebler et al. 2010; Taylor 2012). Thus groundwater
57 management is a complex task requiring multiple tools, including hydrogeological and hydro-
58 chemical models (Healy and Scanlon 2010; Manna et al. 2016). This in turn often requires
59 exhaustive databases and detailed descriptions of environmental conditions, and/or direct
60 measurements using advanced infrastructures and equipment (Herrmann et al. 2015). In many
61 cases, such resources are not available in developing countries (WWAP 2015). Another
62 approach is to study physical (environmental isotopes) (Barrett et al. 1999; Vystavna et al.
63 2018c) and hydro-chemical (inorganic and organic) tracers (Fenech et al. 2012) that can
64 provide information on groundwater recharge and contamination at a reasonable cost in a
65 short time (Yin et al. 2019). The stable isotopes of water, i.e., oxygen-18 (^{18}O) and deuterium
66 (^2H), have been found to be efficient tracers for describing groundwater recharge, water
67 origin, age, and pathways (Ettayfi et al. 2012; Tipple et al. 2017). The stable isotopes of
68 nitrate (^{18}O and ^{15}N) have been widely applied to trace nitrate (NO_3) contamination sources
69 (Urresti et al. 2015; Archana et al. 2018; Taufiq et al. 2019). Organic compounds, particularly
70 pharmaceuticals, have been used to determine the sewage contribution to groundwater
71 (Schaidler et al. 2016; McCance et al. 2018; Castiglioni et al. 2019). However, a multi-tracing
72 approach that includes physical, organic, and inorganic chemical tracers for assessing the
73 urban water cycle has not been fully investigated. For example, a combination of these
74 methods has not been used previously to identify recharge and contamination seasonality in
75 shallow alluvial aquifers located in a temperate climate. Thus the present study had the
76 following objectives: (i) to describe recharge conditions in urban and forest groundwater

77 catchments; (ii) to evaluate hydro-chemical parameters and stable isotopes in groundwater;
78 and (iii) to trace and quantify mixing of groundwater with sewage and tap water leaks.

79 The novelty of the research lies in the sophisticated application of multiple tracers
80 (stable isotopes of water and nitrates, conventional hydro-chemical parameters, and emerging
81 pollutants) in parallel with conventional approaches (hydro-geochemical models, multivariate
82 statistics) to determine the seasonality of groundwater recharge and contamination with water
83 and land uses. In the study, urban and natural (forested) groundwater catchments (located in
84 presumably similar climate and hydro-geological settings) were compared. The study area
85 was the densely populated city of Kharkiv (1.4 million inhabitants) in Eastern Ukraine, where
86 groundwater is used as an alternative to tap water (Vystavna et al. 2017). The study area has
87 limited local runoff and is located in a zone under risk of military action. Therefore,
88 groundwater is considered an important strategic drinking water source that can potentially
89 replace tap water in an emergency. The shallow aquifer selected for the analysis has been
90 studied previously in terms of general contamination status and hydrogeological conditions
91 (Yakovlev et al. 2015; Vystavna et al. 2017), but knowledge of the seasonality of recharge
92 and water quality variation in the aquifer was lacking.

93 2. Studied catchments

94 Five urban (T1, S2, N3, Y4, and P5) and one peri-urban forested (O6) groundwater
95 sites were selected for this study. All sites are located in the forest-steppe zone of the
96 temperate continental climate area, with average annual precipitation of 521 mm and average
97 annual air temperature of +9.1°C (2005-2017; Kharkiv airport World Meteorological
98 Organization (WMO) station, ID 34300). During the sampling period (October 2016-
99 September 2017), total precipitation was 18% lower (426 mm) than the long-term average,
100 indicating a dry hydrological period. Cold season precipitation (November-April) accounted

101 for ~70% of total precipitation during the sampling period. From April to October (warm
102 season), evapotranspiration usually exceeds precipitation in the region.

103 Groundwater was studied where it emerges at the surface as springs (Figure 1a). The
104 urban springs were fitted with outflow tubes and the forest spring flowed into an open pit
105 discharging outflowing groundwater. The maximum elevation at the spring outflows ranged
106 from 113-123 m a.s.l. in the urban catchment to 140 m a.s.l. in the forested catchment. The
107 most recent sediment layers (up to 120 m thick) are composed predominantly of permeable
108 materials (sands and loams) of Quaternary, Neogene, and Paleogene origin, but with some
109 spot inclusions of clay in upper layers (Geological Survey 2007). Springs are fed from
110 fractured fine-grained sandstones and siltstones of the Eocene age. The depth to the aquifer is
111 2-36 m below the surface and the average hydraulic conductivity of the saturated zone is
112 $2 \times 10^{-4} \text{ m s}^{-1}$. The aquifer can be considered a homogeneous system in which the watertable is
113 adapted to the topography and is recharged by precipitation and anthropogenic sources
114 (Geological Survey 2007; Vystavna et al. 2017). Hydrogeological cross-sections are shown in
115 Supplementary Material.

116 The land uses in Kharkiv city (total area 307 km²), where the five urban springs (T1-
117 P5) are located, include residential (55% of total area), industrial (16.5%), vegetated areas
118 (20%), and traffic networks. The population density is 3200-27,400 per km² (for details, see
119 Supplementary Material). The urban water supply is provided predominantly (97%) by two
120 sources of surface water: (i) the Seversky Donets River, around 40 km from the city (85% of
121 the total drinking water supply) and (ii) the man-made Dnipro-Donbass channel, starting
122 around 130 km from the city and carrying water from the Dnipro River to the Seversky
123 Donets River basin. Two water treatment plants are located within the urban area. The
124 centralized drinking water supply from deep groundwater wells (up to 800 m depth)
125 comprises just 3% of the total supply and is limited to two small neighborhoods (18,200

126 inhabitants; 6.64 km²) not located within the study area. Pressurized water supply pipes are
127 placed at 0-5 m below the terrain. Urban wastewater is collected by shallow and deep mains,
128 and undergoes mechanical and biological treatment at the city's wastewater treatment plant
129 (WWTP) (550,000 m³ d⁻¹). The treated wastewater is discharged into the Lopan and Udy
130 Rivers (Figure 1a,b). Around 20% of urban households are not connected to the urban
131 sewerage network and instead use pit latrines and septic tanks, which can leak into the
132 shallow groundwater. At present, the sanitary infrastructure in Kharkiv city is in a state of
133 disrepair, resulting in numerous and frequent leaks (around 24% of total water supply), a
134 problem that cannot be eliminated in the short term (KP Voda 2017).

135 Catchment O6 drains a forest-dominated landscape without agricultural land use and
136 only negligible urbanization (residential buildings and roads account for <9% of the total
137 drained area). The forest vegetation is typical forest-steppe oak woodlands on a rolling plain
138 terrain with grey and dark-grey forest soils. Besides forestry, catchment O6 is used mainly for
139 outdoor recreation.

140 **3. Methods**

141 **3.1 Meteorological and hydrogeological parameters**

142 Meteorological data (daily air temperature, relative humidity, precipitation) for the
143 period 2015-2017 were obtained from Kharkiv WMO station. Potential pan
144 evapotranspiration was calculated based on mean monthly air temperature and humidity,
145 according to a method adapted by Romanenko (1961) for the climate and soil conditions of
146 Ukraine.

147 Spring catchment areas were delineated according to upstream boundaries of water
148 lines measured on local hydrogeological maps (Geological Survey 2007). The remaining
149 uncertainty in groundwater flow direction was handled by including a 20° shift of the

150 auxiliary water flow line on both sides, as proposed by Ferrante et al. (2015).

151 Minimum water transit time was estimated based on the velocity of vertical infiltration
152 flow at the spring outflows, taking into account the thickness of upper sediment layers and the
153 hydraulic conductivity of the vadose zone. Maximum water transit time was estimated based
154 on the velocity of the lateral groundwater flow at the most remote catchment area boundary,
155 considering the orography, groundwater flow direction, and hydrogeological structures
156 (Geological Survey 2007). Detailed calculations are presented in Supplementary Material.

157 **3.2 Sampling and analysis**

158 Monthly precipitation (October 2015-September 2017) was sampled at the Kharkiv
159 Global Network of Isotopes in Precipitation (GNIP) station (49.5615°N/36.1208°E, 101 m
160 a.s.l., located 3 km from Kharkiv WMO station) coordinated by the International Atomic
161 Energy Agency (IAEA), using a commercial evaporation-free precipitation collector with a
162 submerged capillary tube (PALMEX®, Croatia). Groundwater was sampled monthly for
163 hydrological variables and stable isotopes of water, and on five occasions from October 2016
164 to September 2017 for hydro-chemical parameters. Discharge in springs was measured at the
165 time of sampling, using a stopwatch and a calibrated container. Simultaneously, groundwater
166 temperature was measured using a mercury thermometer, while pH, electrical conductivity
167 (EC), and redox potential (ORP) were measured using HI-98130 Multiparameter and H-
168 98121 Pocket pH and ORP tester (Hanna Instruments®).

169 Tap water samples were collected from two drinking water supply schemes. The first
170 site represented the part of urban tap water network supplied by the Dnipro-Donbass channel
171 (one sample in October 2016). The second represented the part of the network where water
172 comes from the Seversky Donets River (six bi-monthly samples October 2016-September
173 2017) (Figure 1b). The purpose was to check whether tap water of different origins had

174 similar isotopic composition. A sample of the sewage influent to the WWTP was taken
175 simultaneously with the tap water sample in September 2017, in order to compare their
176 isotopic composition (Figure 1b).

177 Unfiltered water samples for analysis of major ions and nitrate were collected in 500-
178 mL plastic bottles and analyzed by the potentiometric method (Vystavna et al. 2017). The
179 difference between two replicates was less than 5%. For analysis of stable isotopes of water
180 ($\delta^{18}\text{O-H}_2\text{O}$ and $\delta^2\text{H-H}_2\text{O}$), water samples were collected in 50-mL high-density polyethylene
181 bottles and analyzed using the laser instrument Picarro L2120-*i*. Each sample was analyzed at
182 least twice, with seven injections per vial. The results were compared with those for internal
183 laboratory standards calibrated against primary reference materials, and were expressed per
184 mille (‰) relative to the Vienna Standard Mean Ocean Water (V-SMOW). The typical
185 precision, expressed as the one-year variance in an internal control standard, didn't exceed
186 $\pm 0.1\text{‰}$ and $\pm 1.0\text{‰}$ for $\delta^{18}\text{O-H}_2\text{O}$ and $\delta^2\text{H-H}_2\text{O}$, respectively.

187 Water samples for analysis of stable isotopes of nitrate ($\delta^{15}\text{N-NO}_3$ and $\delta^{18}\text{O-NO}_3$) were
188 collected in October 2016 and September 2017. These samples were filtered (0.22 μm) in the
189 field and transferred to plastic bottles (50 mL). Nitrate isotope analysis was carried out by the
190 denitrifier method (Sigman et al. 2001; Casciotti et al. 2002), whereby nitrate was converted
191 to N_2O and an isotope ratio mass spectrometer (GasbenchII/delta V plus, Thermo Fisher
192 Scientific®, USA) is used for simultaneous determination of $\delta^{15}\text{N-NO}_3$ and $\delta^{18}\text{O-NO}_3$. The
193 results were compared with those for internal laboratory standards calibrated against primary
194 reference materials, and were expressed as ‰ relative to the standards AIR for $\delta^{15}\text{N-NO}_3$ and
195 V-SMOW for $\delta^{18}\text{O-NO}_3$. Typical precision, expressed as the one-year variance in an internal
196 control standard, was better than $\pm 0.6\text{‰}$ for $\delta^{15}\text{N-NO}_3$ and $\pm 0.4\text{‰}$ for $\delta^{18}\text{O-NO}_3$.

197 Groundwater samples (1-L amber glass bottles) for non-targeted analysis of emerging
198 compounds were collected in September 2017. The screening of chemicals was based on an
199 exact mass in an open access library (over 2,000 compounds) by liquid chromatography
200 quadrupole time-of-flight mass spectrometry (LS-Q-TOF-MS) coupled to an Accela 1250 LC
201 pump (Thermo Fisher Scientific®) and an HTS XT-CTC autosampler (CTC Analytics AG®,
202 Switzerland), operated using Xcalibur software (Thermo Fisher Scientific®). A Hypersil gold
203 aQ column (50 mm × 2.1 mm ID × 5 µm particles; Thermo Fisher Scientific®) was used for
204 chromatographic separation. Details of sample preparation can be found in Supplementary
205 Material.

206 Results on the presence of the most likely compounds were selected according to the
207 following criteria: i) error between theoretical and experimental exact mass <5 ppm; ii)
208 difference in isotopic pattern between theoretical and experimental <10%; iii) identification of
209 the compounds using comparison of the spectrum obtained with the theoretical spectrum,
210 based on the exact mass library with probability >70% (Library Score), where the score takes
211 into account the isotopic distribution, mass accuracy, and mass/spectra, with values close to
212 100 showing the most likely elemental composition; and iv) retention time (error <5%).
213 Because of the nature of the screening analysis, exact concentrations could not be determined.

214 **3.3 Data analyses**

215 The relative ion composition for each sampling site was plotted in diagrams according
216 to Stiff (1951) and the isometric log-ratio (ilr)-ion according to Shelton (2018). The
217 environmental data were tested for normal distribution. When the distribution was skewed,
218 the data were transformed logarithmically (Legendre and Legendre 2012). Principal
219 component analysis (PCA) was used to plot isotope and hydro-geochemical characteristics per
220 site and month. In a second PCA with time-averaged isotope and hydro-geochemical

221 characteristics per site, the presence/absence in the springs of a range of emerging organic
222 compounds, such as drugs, pesticides, and food compounds from one-off measurements, was
223 fitted using the procedure “envfit” (Oksanen et al. 2018). All calculations were performed in
224 R 3.3.5 (R Core Team 2018). Detailed information on the statistical analyses is provided in
225 Supplementary Material.

226 The local meteoric water line (LMWL) (October 2015-September 2017, n=24) was
227 constructed by the reduced major axis method (Crawford et al. 2014). The equation obtained
228 was compared with the global meteoric water line (GMWL), described as $\delta^2\text{H} = 8 \times \delta^{18}\text{O} + 10$
229 by Craig (1961). Isotopic composition of springs, sewage, and tap water was plotted against
230 the LMWL, to examine relative variation and differences in isotopic composition of
231 hydrological components. Deuterium excess (d-excess = $\delta^2\text{H} - 8 \times \delta^{18}\text{O}$) was used as an
232 indicator of non-equilibrium conditions, which occur during evaporation as water with d-
233 excess <10‰ is presumed to undergo evaporation (Dansgaard 1964).

234 A two-component mixing model (Unnikrishna et al. 2002) was used to estimate the
235 contribution of precipitation from warm (May-October) and cold (November-April) periods
236 of the year, based on annual flow-weighted $\delta^{18}\text{O}\text{-H}_2\text{O}$ value in springs and in cold and warm
237 precipitation (calculations shown in Supplementary Material).

238 The groundwater transit time was estimated according to Herrmann et al. (2015):

$$239 \quad \tau_r = \frac{\sqrt{\frac{1}{f^2} - 1}}{2\pi} \quad (1)$$

240 where τ_r is the groundwater transit time in years and f is the ratio of $\delta^{18}\text{O}\text{-H}_2\text{O}$ amplitude in
241 groundwater flow to that in precipitation. The transit time was estimated by two approaches:
242 (i) using the amplitude of $\delta^{18}\text{O}\text{-H}_2\text{O}$ for the 12-month study period; and (ii) using the
243 amplitude of $\delta^{18}\text{O}\text{-H}_2\text{O}$ taken only for the cold period, assuming selective recharge (Vystavna
244 et al. 2018c). A first rough approximation of groundwater transit time at the study sites was

245 calculated assuming that the isotopic lapse rate was insignificant due to the small differences
 246 in elevation between catchments.

247 The chloride (Cl^-) concentration and $\delta^{18}\text{O}\text{-H}_2\text{O}$ were used to separate the annual
 248 contributions of tap water and sewage leaks to urban groundwater, using the ternary mixing
 249 model (Grimmeisen et al. 2017; Vystavna et al. 2018d):

$$250 \quad (f_1+f_2+f_3) \times [\text{Cl}^-, \delta^{18}\text{O}]_{\text{ub}} = f_1 \times [\text{Cl}^-, \delta^{18}\text{O}]_{\text{gw}} + f_2 \times [\text{Cl}^-, \delta^{18}\text{O}]_{\text{tw}} + f_3 \times [\text{Cl}^-, \delta^{18}\text{O}]_{\text{sw}} \quad (2)$$

251 where Cl^-_{ub} and $\delta^{18}\text{O}_{\text{ub}}$ [mg L^{-1} , ‰] are flow-weighted chloride concentration and $\delta^{18}\text{O}\text{-H}_2\text{O}$
 252 in urban springs; Cl^-_{gw} and $\delta^{18}\text{O}_{\text{gw}}$ [mg L^{-1} , ‰] are flow-weighted chloride concentration and
 253 $\delta^{18}\text{O}\text{-H}_2\text{O}$ in the forest spring; Cl^-_{tw} and $\delta^{18}\text{O}_{\text{tw}}$ [mg L^{-1} , ‰] are average chloride
 254 concentration and $\delta^{18}\text{O}\text{-H}_2\text{O}$ in tap water; and Cl^-_{sw} and $\delta^{18}\text{O}_{\text{sw}}$ [mg L^{-1} , ‰] are chloride
 255 concentration and $\delta^{18}\text{O}\text{-H}_2\text{O}$ in sewage. Chloride concentration in sewage was considered
 256 stable and equal to the average of 350 mg L^{-1} (City Council 2010). The $\delta^{18}\text{O}\text{-H}_2\text{O}$ in tap water
 257 was used for sewage, assuming similar origin of these waters (Vystavna et al. 2018d). The
 258 values f_1 , f_2 , and f_3 are the fractions of natural recharge, water supply, and sewage leaks,
 259 respectively, with the sum of f_1 , f_2 and f_3 equal to 1.

260 To separate seasonal contribution of sewage leaks (f_1) from other possible recharge
 261 sources (f_2), measured $\delta^{18}\text{O}\text{-H}_2\text{O}$ and Cl^- concentration were used as tracers in the binary
 262 model (Vystavna et al. 2018d):

$$263 \quad (f_1+f_2) \times [\text{Cl}^-, \delta^{18}\text{O}]_{\text{ub}} = f_1 \times [\text{Cl}^-, \delta^{18}\text{O}]_{\text{sw}} + f_2 \times [\text{Cl}^-, \delta^{18}\text{O}]_{\text{gw}} \quad (3)$$

264 The simultaneous use of Cl^- and $\delta^{18}\text{O}\text{-H}_2\text{O}$ enabled differentiation between inputs from
 265 sewage and road de-icing salt. Both these sources have a high chloride content, but de-icing
 266 salt enters the groundwater mainly with snowmelt, which has lower isotopic signature than
 267 sewage. Moreover, street runoff is mostly collected by the urban drainage and storm water
 268 system. Binary and ternary models were processed using the MIX Program v1.0 (Vázquez-

269 Suñé et al. 2010). The $\delta^{15}\text{N}\text{-NO}_3$ vs. $\delta^{18}\text{O}\text{-NO}_3$ linear regression plot was used to determine
270 the dominant sources of nitrate in groundwater (Kendall 1998).

271 **4. Results**

272 **4.1 Stable isotopes of water in precipitation**

273 Between October 2015 and September 2017, the isotope concentrations in
274 precipitation were highly variable, with extreme lows in November 2016. The amount-
275 weighted average $\delta^{18}\text{O}\text{-H}_2\text{O}$ and $\delta^2\text{H}\text{-H}_2\text{O}$ in precipitation was -9.2‰ and -64.5‰ ,
276 respectively. Annual amplitude of $\delta^{18}\text{O}\text{-H}_2\text{O}$ and $\delta^2\text{H}\text{-H}_2\text{O}$ in precipitation was 8.7‰ and
277 63.3‰ , respectively (details in Supplementary Material). On a monthly scale, the oxygen and
278 hydrogen stable isotopes in precipitation correlated well with average annual air temperature
279 (Pearson coefficient $r > 0.77$, $p < 0.01$, $n = 24$), but not with precipitation amount ($r < 0.5$). The
280 equation obtained for the LMWL was: $\delta^2\text{H} = 7.61 \times \delta^{18}\text{O} + 4.88$.

281 The urban sites T1 and Y4 and the forest site O6 had relatively similar isotopic range,
282 but differing d-excess values (7.1‰ , 9.9‰ , and 8.4‰ , respectively). Site N3 showed slightly
283 higher isotopic values than the group of urban springs. Site S2 had the lowest and site P5 the
284 highest isotopic values among the springs (Figure 2). According to the simultaneously taken
285 samples, tap water from the Dnipro-Donbass channel was slightly enriched in isotopes
286 compared with tap water from the Seversky Donets River. The isotopic composition of tap
287 water was more seasonally variable than that of groundwater, with lower d-excess values and
288 higher isotopic values, giving a regression line with a clear evaporation signal reflecting the
289 surface water origin. The isotopic values of S2, N3, and P5 were well aligned with the tap
290 water regression line (Figure 2). Simultaneously taken samples of sewage and tap water had
291 similar isotopic composition, with standard deviation $< 5\%$.

292 **4.2 Precipitation contribution and groundwater transit time**

293 The annual amplitude of $\delta^{18}\text{O}\text{-H}_2\text{O}$ in groundwater differed slightly between sites,
 294 ranging from 0.1‰ to 0.3‰. The contribution of warm and cold precipitation to groundwater
 295 recharge was comparable between springs, with a marked dominance (>83%) of cold
 296 precipitation. Groundwater transit time was comparable for sites N3, Y4, P5, and O6, but
 297 slightly shorter for S2 and twice as long for site T1 (Table 1).

298 Table 1. Precipitation contribution, groundwater transit time, and recharge at the five urban
 299 sites (T1, S2, N3, Y4, and P5) and the forest site (O6)

Site ID	Cold precipitation contribution %	Warm precipitation contribution %	Groundwater transit time, years				Estimated recharge		
			Hydro-geological method (based on filtration and recharge area)	Isotopic method based on:		According to the position of extreme $\delta^{18}\text{O}\text{-H}_2\text{O}$ values	Natural recharge f_1 , %	Recharge by tap water leaks f_2 , %	Recharge by sewage leaks f_3 , %
				Annual amplitude of $\delta^{18}\text{O}\text{-H}_2\text{O}$	Amplitude of $\delta^{18}\text{O}\text{-H}_2\text{O}$ in the cold period				
T1	89	11	0.4–26	14	1.7	Not detectable	76	0	24
S2	93	7	0.9–18	5	0.6	0.7	89	8	3
N3	87	13	0.3–4.7	7	0.8	0.8	70	13	17
Y4	91	9	0.3–3.3	7	0.8	Not detectable	82	4	14
P5	83	17	0.3–3.8	5	0.7	0.7	55	34	11
O6	90	10	0.3–5.1	7	0.7	0.7*	100*	0*	0*

300 *Assumed according to the position of the extreme isotopic value and selected calculation method.

301 4.3 Major ion composition

302 The groundwater was near neutral or slightly acidic, with pH values between 6.1 and
 303 7.4. Redox potential ranged from oxidizing to reducing conditions (from +287 to -117 mV),
 304 while EC varied between 950 and 1540 $\mu\text{S cm}^{-1}$ in the urban springs, but was lower (740 to
 305 900 $\mu\text{S cm}^{-1}$) in the forest spring. Total dissolved solids (TDS) ranged from 861 to 1170
 306 mg L^{-1} in the urban springs and from 632 to 732 mg L^{-1} in the forest spring. HCO_3^-
 307 concentration ranged from 230 to 480 mg L^{-1} in both urban and forest springs. Average Cl
 308 concentration in urban springs ($74\pm 30 \text{ mg L}^{-1}$) was approximately twice that in the forest
 309 spring ($25\pm 14 \text{ mg L}^{-1}$). Average SO_4^{2-} and Na^+ concentrations were notably higher (280 ± 100
 310 mg L^{-1} and $124\pm 35 \text{ mg L}^{-1}$, respectively) in urban springs than in the forest spring (65 ± 10

311 mg L^{-1} and $39 \pm 3 \text{ mg L}^{-1}$, respectively). The Ca^{2+} , Mg^{2+} , and K^{+} concentrations were
312 comparable between urban and forest springs (Figure 3a). However, HCO_3^{-} and SO_4^{2-} were
313 the dominant ions in the urban springs, while HCO_3^{-} and Ca^{2+} dominated in the forest spring
314 (Figure 3a). Tap water had highly variable ion concentrations, particularly for HCO_3^{-} , Cl^{-} ,
315 SO_4^{2-} , and Na^{+} (Figure 3a). Its dominant ion composition was comparable to that of urban
316 groundwater. Sewage was characterized by higher SO_4^{2-} , Cl^{-} , and Na^{+} concentrations
317 compared with groundwater and tap water (Figure 3a). Samples from the forest spring O6,
318 and to a lesser degree from urban spring Y4 and tap water, were of the HCO_3^{-} type. Sewage,
319 and to a lesser extent urban spring S2, tap water, and then springs N3 and T1, were of the Na^{+}
320 + K^{+} type. The samples were best distinguished based on the ratio $\text{Cl}^{-} + \text{SO}_4^{2-}$ to HCO_3^{-}
321 (Figure 3b). The measured variables are shown in Supplementary Material.

322 Multivariate statistical analysis showed that, in terms of isotope and hydro-chemical
323 water composition, the springs T1, N3, Y4, and P5 were also similar over time, with gradually
324 increasing EC from Y4 to P5, N3, and T1 (Figure 4). In contrast, the forest spring O6 plotted
325 separately, towards the lowest concentrations of ions and EC. Urban spring S2 plotted at
326 another extreme, with the lowest isotope ratios and the highest concentrations of inter-
327 correlated SO_4^{2-} and Na^{+} . Tap water was even farther along the first axis, which was mostly
328 positively correlated with EC and TDS. Thus, the general order was: tap water, the natural
329 spring O6, urban springs Y4 and S2, then P5 and T1, and finally N3 (Figure 4).

330 **4.4 Nitrate contamination, contribution of sewage and tap water leaks**

331 Nitrate concentrations showed high variability, ranging from 0.3 to 90 mg L^{-1} in the
332 urban springs and from 0.3 to 7 mg L^{-1} in the forest spring, and with noticeable NO_3^{-}
333 enrichment (5- to 10-fold) in urban groundwater. Except at site T1, the maximum nitrate
334 concentrations were observed in March and June (Figure 5). Stable isotopes of nitrate in the

335 springs were within the range reported for NO_3^- derived from sewage and manure (Figure 6).
336 Sites T1 and Y4 displayed high variation in $\delta^{18}\text{O}-\text{NO}_3$. However, the variation in $\delta^{15}\text{N}-\text{NO}_3$
337 values was lower at all sites. At most urban springs (T1, N3, Y4, and P5), stable isotopes of
338 nitrate, particularly $\delta^{18}\text{O}-\text{NO}_3$, tended towards enrichment with increasing NO_3^- concentration
339 (Figure 6).

340 The sewage contribution at sites T1 and N3 was estimated to be 19-24% and showed
341 less seasonal variation than in the other urban springs (Figure 5). At sites Y4 and P5, the
342 sewage contribution was lowest in October 2016 and highest in December 2016. At P5, the
343 sewage contribution was positively related to discharge. At site S2, the sewage contribution
344 was less than 3% (Figure 5). The annual contribution of tap water leaks to urban groundwater
345 recharge was highly variable between sites, with the maximum estimated for P5 (34%). Site
346 S2 showed the lowest recharge from sewage and tap water leaks among the urban springs
347 (Table 1).

348 **4.5 Emerging contaminants in groundwater**

349 The emerging contaminants detected in groundwater were divided into three groups:
350 drugs (caffeine, nikethamide, riluzole, phenazone, pilocarpine, pergolide, ajmaline,
351 carbamazepine, moxonidine, dihydrocodeine, sulfathiazole, papaverine, and aripiprazole),
352 pesticides (DEET (pentedrone), dodine, chlordimeform, atrazine, simazine, and butraline),
353 and food compounds (alternariol (a mycotoxin), chanoclavine and kojic acid (food additives)
354 (details of use and properties are shown in Supplementary Material). All of the drugs detected
355 can be abused and some are illicit drugs. The most frequently detected drug (in five of the six
356 springs studied) was the alkaloid pilocarpine, which was found even in the forest spring.
357 Chanoclavine and chlordimeform were detected in four springs. Caffeine, phenazone, and
358 alternariol were found in three springs. Other compounds were found at one or two sites. Each

359 spring was characterized by a distinct group of detected compounds according to the PCA
360 ordination (Figure 7). The stimulant caffeine and food compounds tended towards the positive
361 y axis and correlated well with Na^+ and SO_4^{2-} . Four pesticides and most of the drugs detected
362 tended towards the negative x axis and correlated well with $\delta^{15}\text{N-NO}_3$, Cl^- , and NO_3^- . Atrazine
363 and pilocarpine were more along the positive x axis (Figure 7).

364 5. Discussion

365 5.1 Urban groundwater recharge

366 By complementing hydrogeological modeling with tracing of stable isotopes in water,
367 we were able to delineate natural and anthropogenic recharge of the shallow aquifer studied.
368 The results indicate that both urban and forest springs in the study area are selectively
369 recharged by cold precipitation (Table 1). This is typical for the temperate continental climate,
370 where evapotranspiration can be 2- to 3-fold higher than precipitation amount, which reduces
371 natural recharge during the warm period (Vystavna et al. 2018c). Consequently, the $\delta^{18}\text{O-H}_2\text{O}$
372 amplitude in cold precipitation was found to be a more realistic parameter for estimating
373 groundwater transit time than the amplitude in annual precipitation (Table 1), and this might
374 apply to other sites with a continental climate. In some springs (S2, N3, and P5), the estimated
375 transit time was similar to that determined from naturally occurring isotopic extremes (Table
376 1). Exceptionally low isotopic composition of precipitation in November 2016 was associated
377 with isotopically depleted Arctic air masses and locally recycled moisture exceeding
378 evaporation according to the Hybrid Single Particle Langarian Integrated Trajectory model
379 (details in Supplementary Material). With its high amount, combined with above-zero air
380 temperature and low evapotranspiration, November precipitation was efficient in recharging
381 groundwater, which explains the unusually low isotopic composition in some urban springs

382 (S2, N3, and P5) (Figure 5). Therefore, natural $\delta^{18}\text{O}\text{-H}_2\text{O}$ extremes in precipitation were used
383 as natural tracers to confirm the estimated groundwater transit time (Table 1).

384 The hydrogeological method for estimating groundwater transit time cannot be highly
385 accurate due to limited availability of hydrogeological data (Healy and Scallion 2010).
386 However, it gives a preliminary range of the possible water age in the aquifer. Our findings
387 confirm the validity of the model used (Eq.1) in estimating regional groundwater transit time,
388 and also highlight potential applications of isotopic extremes in hydrogeological studies.

389 Since isotopic and chemical signatures differed between hydrological components, it
390 was possible to estimate anthropogenic recharge by applying binary and ternary mixing
391 models. In the present case, tap water and sewage had lower d-excess than warm
392 precipitation, indicating that likely mixing with tap water and sewage decreased the d-excess
393 of urban springs compared with the natural recharge conditions (Figure 2). We found a
394 discrepancy between the contributions of precipitation, tap water, and sewage leaks,
395 signifying that natural recharge of springs in Kharkiv city can be limited to large hydrological
396 events occurring in the cold period (Table 1). Similar mechanisms can be expected to operate
397 in other temperate, dry-summer areas with inadequate water management. Tap water and
398 sewage leaks have been found to contribute to urban groundwater recharge, changing the
399 hydrological function of groundwater and influencing its contamination status, as found in
400 many previous studies (Chen et al. 2008; Houhou et al. 2010; Tubau et al. 2017). The method
401 for quantification of tap water leaks into groundwater applied in the present study was based
402 in principle on distinct isotopic signatures of urban hydrological components that are
403 generally valid for regions where drinking water supply derives from surface water. Thus, this
404 method should generally be applicable to many regions in Eastern and Central Europe,
405 particularly in post-Soviet countries (Moldova, Ukraine, Belarus, and Russian Federation)
406 with similar problems in urban water resource management.

407 **5.2 Urban groundwater contamination**

408 Isotope composition and changes in this over time clearly distinguished the forest
409 spring from urban groundwater, but stable isotopes of water were not able to trace
410 groundwater contamination and its origin. However, the additional chemical variables
411 measured (EC, TDS, Cl^- , Na^+ , and NO_3^- concentrations) revealed the influence of
412 anthropogenic activities in urban springs (Figures 3a and 6). This confirms findings in other
413 studies in different regions (Schmidt et al. 2007; Ettayfi et al. 2012; Grimmeisen et al. 2017).
414 The general hydro-chemical trend in our study was from the forest spring O6 to urban sites
415 Y4 and S2, further to sites P5 and T1, and then N3 (Figure 4). Spatially and seasonally highly
416 variable nitrate contamination (Figure 5) was likely controlled by different nitrate source and
417 hydrological processes. Nitrate in soil can originate from leaky pit latrines and septic tanks,
418 but also from soil nitrification (Nikolenko et al. 2018). At sites T1 and S2, the nitrate
419 concentration decreased with increasing flow, indicating dilution. In the other springs,
420 including that at the forest site, the nitrate concentration increased with increasing flow
421 (Figure 5). A reason may be that oversaturated soil can release accumulated nitrate when the
422 water level changes. Ensuing nitrate contamination in groundwater has been observed e.g., in
423 Western France (Aquilina et al. 2012). In the present study, analysis of stable isotopes of
424 nitrate confirmed that sewage leaks can be the principal source of nitrate accumulation in the
425 soil (Figure 6), as we also found in an earlier study (Vystavna et al. 2017). Mineralization and
426 subsequent nitrification of the organic soil N-pool could be a source of nitrate, particularly at
427 the forest site, but it was not clearly distinguished in the $\delta^{15}\text{N}\text{-NO}_3$ vs. $\delta^{18}\text{O}\text{-NO}_3$ bi-plot
428 (Figure 6). Without additional tracers (e.g., boron; Kendall 1998), stable isotopes of nitrate
429 are not able to discriminate manure, which can be a nitrate source in the forest catchment
430 (dumping of animal excrement) and at site P5 (potential leaks from a zoological park).
431 However, sewage leaks were traceable by human drugs and food compounds in urban springs

432 (Figure 7). The highest diversity of drugs and food compounds was found in those springs
433 that also showed the highest sewage contribution (T1, N3, Y4, and P5). The relationship
434 observed between the non-persistent chemicals caffeine and food compounds, and some ions
435 (SO_4^{2-} and Na^+) indicates that these emerging compounds continually enter T1 with raw
436 sewage, likely from mains. However, the positive relationship between persistent drugs,
437 pesticides, and NO_3^- at N3, Y4, and P5 may point to sewage leaks from pit latrines rather than
438 sewage mains (Figure 7). Some persistent pesticides and food compounds were detected at
439 sites with negligible sewage contribution (urban site S2 and forest site O6). This suggests
440 accumulation over time (Jurado et al. 2012).

441 Overall, our results indicate that organic tracers can be useful in confirming sewage
442 contribution to urban groundwater, but also in differentiating raw sewage inputs from those
443 derived from pit latrines and septic tanks. The resulting influence on groundwater quality
444 threatens its usability as a drinking water source (Schmidt et al. 2017) and likely influences
445 the biotic community (Di Lorenzo et al. 2019). These will be considered as additional
446 indicators of urban impact in our future research.

447 6. Conclusions

448 By combining stable isotopes of water with hydrogeological calculations, we were
449 able to describe recharge conditions in urban and forest groundwater catchments that clearly
450 indicate strong seasonal patterns of groundwater, to evaluate groundwater contamination in
451 urban areas, and to quantify mixing of groundwater with sewage and tap water leaks. Data on
452 emerging compounds supported our conclusions on spatially distinct types of anthropogenic
453 recharge and helped to distinguish between contamination of urban groundwater with raw
454 sewage from defective mains and with leaks from pit latrines and septic tanks. Since
455 groundwater, particularly at shallow depth, can be heavily influenced by seasonal patterns of

456 recharge and land use, seasonal monitoring is important (or even essential) in order to reach
457 useful conclusions on the patterns shaping water quality and thus the usability as a drinking
458 water resource. High nitrate contamination of urban springs and the presence of potentially
459 toxic emerging compounds indicate health risks associated with the use of the urban springs
460 studied as drinking water sources. This poses crucial challenges for future planning of
461 resource allocation.

462 Combining physical (isotopes) and chemical (major ions and emerging compounds)
463 analyses proved useful in determining and quantifying hydrological and hydro-chemical
464 processes in the urban subsurface. This multi-tracing method provides an integrative and
465 comprehensive view of the regional hydrological cycle, which can be helpful for improving
466 urban water management. Having been tested in a major Eastern European city, the proposed
467 tool can be particularly useful for cities suffering from similar problems of poor water
468 management and inadequate sewage and water supply infrastructure.

469 **Acknowledgements**

470 This research was carried out within the framework of CRP F33024 “Isotope
471 Techniques for the Evaluation of Water Sources for Domestic Supply in Urban Areas” funded
472 by the IAEA and the United Nations Educational, Scientific and Cultural Organization
473 (UNESCO) IHP Program on Emerging Pollutants in Wastewater Reuse in Developing
474 Countries, International Initiative on Water Quality (IIWQ) case study “Emerging pollutants
475 in water and wastewater of East Ukraine: Occurrence, Fate and Regulation” (Contract No.
476 4500282119). The authors thank Dr. Josef Hejzlar for valuable comments.

477 **References**

478 Aquilina L., Vergnaud-Ayraud V., Labasque T., Bour O., Molénat J., Ruiz L., de Montety V.,
479 De Ridder J., Roques C., Longuevergne L., 2012. Nitrate dynamics in agricultural

- 480 catchments deduced from groundwater dating and long-term nitrate monitoring in surface-
481 and groundwaters. *Science of the Total Environment* 435–436, 167–178.
- 482 Archana A., Thibodeau B., Geeraert N., Xu M.N., Kao S.-J., Baker D.M., 2018. Nitrogen
483 sources and cycling revealed by dual isotopes of nitrate in a complex urbanized
484 environment. *Water Research* 142, 459–470.
- 485 Barrett M.H., Hiscock K.M., Pedley S., Lerner D.N., Tellam J.H., French M.J., 1999. Marker
486 species for identifying urban groundwater recharge sources: a review and case study in
487 Nottingham, UK. *Water Research* 33 (14), 3083–3097.
- 488 Casciotti K.L., Sigman D.M., Hastings M.G., Böhlke J.K., Hilkert A., 2002. Measurement of
489 the oxygen isotopic composition of nitrate in seawater and freshwater using the denitrifier
490 method. *Analytical Chemistry* 74, 4905–4912.
- 491 Castiglioni S., Davoli E., Riva F., Palmiotto M., Camporini P., Manenti A., Zuccato E., 2018.
492 Mass balance of emerging contaminants in the water cycle of a highly urbanized and
493 industrialized area of Italy. *Water Research* 131, 287–298.
- 494 Chen Q., Qu J., Liu R., Li W., 2008. Rule-based model for aging-induced leakage from water
495 supply pipe network in Beijing City. *China Water & Wastewater* 24(11), 52–56 (in
496 Chinese with English abstract).
- 497 City Council, 2010. The declaration of the Kharkiv City Council No. 321 from 8.09.2010 on
498 the discharge of raw wastewater in the municipal sewage system.
- 499 Craig H., 1961. Isotopic variations in meteoric waters. *Science* 133, 1702–1703.
- 500 Crawford J., Hughes C.E., Lykoudis S., 2014. Alternative least squares methods for
501 determining the meteoric water line, demonstrated using GNIP data. *Journal of Hydrology*
502 519 (Part B), 2331–2340.
- 503 Dansgaard W., 1964. Stable isotopes in precipitation. *Tellus* 16, 436–468.

- 504 Di Lorenzo, T., Di Marzio W.D., Fiasca B., Galassi D.M.P., Korbel K., Iepure S., Pereira J.L.,
505 Reboleira A.S.P.S., Schmidt S.I., Hose G.C., 2019. Recommendations for ecotoxicity
506 testing with stygobiotic species in the framework of groundwater environmental risk
507 assessment. *Science of the Total Environment* 681, 292-304.
- 508 EEA, 2002. Nitrate concentration in groundwater. Retrieved from European Environment
509 Agency: [http://www.eea.europa.eu/data-and-maps/figures/nitrate-concentration-in-](http://www.eea.europa.eu/data-and-maps/figures/nitrate-concentration-in-groundwater)
510 groundwater.
- 511 Ettayfi N., Bouchaou L., Michelot J.L., Tagma T., Warner N., Boutaleb S., Massault M.,
512 Lgourna Z., Vengosh A., 2012. Geochemical and isotopic (oxygen, hydrogen, carbon,
513 strontium) constraints for the origin, salinity, and residence time of groundwater from a
514 carbonate aquifer in the Western Anti-Atlas Mountains, Morocco. *Journal of Hydrology*
515 438–439, 97–111.
- 516 European Commission, 2012: A Blueprint to Safeguard Europe's Water Resources.
517 Communication from the commission to the European parliament, the Council, the
518 European economic and social committee and the committee of the regions. Brussels,
519 Belgium.
- 520 EU WFD, 2000. Directive 2000/60/EC of the European Parliament and of the Council of the
521 23 October 2000: establishing framework for the community action in the field of water
522 policy. *Official Journal of European Commission L327*, 321–371.
- 523 FAO, 2011. The state of the world's land and water resources for food and agriculture
524 (SOLAW) – Managing systems at risk. Food and Agriculture Organization of the United
525 Nations, Rome and Earthscan, London.
- 526 Fenech C., Rock L., Nolan K., Tobin J., Morrissey A., 2012. The potential for a suite of
527 isotope and chemical markers to differentiate sources of nitrate contamination: a review.
528 *Water Research* 46 (7), 2023–2041.

- 529 Ferrante M., Mazzetti E., Fiori A., Burini M., Fioriti B., Mazzoni A., Schirò G., Vacca G.,
530 Brunone B., Meniconi S., Capponi C., 2015. Delineation of Wellhead Protection Areas in
531 the Umbria region. 2. Validation of the Proposed Procedure. *Procedia Environmental*
532 *Sciences* 25, 96–103.
- 533 Geological Survey, 2007. Supplementary report to geological map of Ukraine, scale
534 1:200000, sheets M-37-XIII (Kharkiv). Printed in Kharkiv, Ukraine.
- 535 Grimmeisen F., Lehmann M.F., Liesch T., Goeppert N., Klinger J., Zopfi J., Goldscheider N.,
536 2017. Isotopic constraints on water source mixing, network leakage and contamination in
537 an urban groundwater system. *Science of the Total Environment* 583, 202–213.
- 538 Groundwater Directive, 2006. European Commission, COM(2003)550.
- 539 Healy R.W., Scanlon B.R., 2010. *Estimating Groundwater Recharge*. Cambridge University
540 Press, Cambridge, New York.
- 541 Herrmann F., Keller L., Kunkel R., Vereecken H., Wendland F., 2015. Determination of
542 spatially differentiated water balance components including groundwater recharge on the
543 Federal State level – a case study using the mGROWA model in North Rhine-Westphalia
544 (Germany). *Journal of Hydrology: Regional Studies* 4 (Part B), 294–312.
- 545 Houhou J., Lartiges B.S., France-Lanord C., Guilmette C., Poix S., Mustin C., 2010. Isotopic
546 tracing of clear water sources in an urban sewer: A combined water and dissolved sulfate
547 stable isotope approach. *Water Research* 44 (1), 256–266.
- 548 Jurado A., Vazquez-Sune E., Carrera J., Lopez de Alda M., Pujades E., Barcelo D., 2012.
549 Emerging organic contaminants in groundwater in Spain: a review of sources, recent
550 occurrence and fate in a Europe context. *Science of the Total Environment* 440, 82–94.
- 551 Kendall C., 1998. Tracing nitrogen sources and cycling in catchments. In: Kendall C,
552 McDonnell JJ (eds) *Isotope tracers in catchment hydrology*. Elsevier, Amsterdam, 839 pp.
- 553 Legendre P., Legendre, L., 2012. *Numerical ecology*. Elsevier.

- 554 Manna F., Cherry J.A., McWhorter D.B., Parker B.L., 2016. Groundwater recharge
555 assessment in an upland sandstone aquifer of southern California. *Journal of Hydrology*
556 541 (Part B), 787–799.
- 557 McCance W., Jones O.A.H., Edwards M., Surapaneni A., Chadalavada S., Currell M., 2018.
558 Contaminants of Emerging Concern as novel groundwater tracers for delineating
559 wastewater impacts in urban and peri-urban areas. *Water Research* 146, 118–133.
- 560 Nikolenko O., Jurado A., Borges A., Knoller K., Brouyer S., 2018. Isotopic composition of
561 nitrogen species in groundwater under agricultural areas: A review. *Science of the Total*
562 *Environment* 621, 1415–1432.
- 563 Oksanen F., Blanchet F.G., Friendly M., Kindt R., Legendre P., McGlinn D., Minchin P.R.,
564 O'Hara R. B., Simpson G.L., Solymos P., Stevens M.H.H., Szoecs E., Wagner H., 2018.
565 *Vegan: Community Ecology Package*. R package version 2.5-2. [https://CRAN.R-](https://CRAN.R-project.org/package=vegan)
566 [project.org/package=vegan](https://CRAN.R-project.org/package=vegan).
- 567 R Core Team, 2018. *R: A language and environment for statistical computing*. R Foundation
568 for Statistical Computing, Vienna, Austria. <https://www.R-project.org/>.
- 569 Romanenko V.A., 1961. Computation of the autumn soil moisture using a universal
570 relationship for a large area. *Procedia of the Ukrainian Hydrometeorological Research*
571 *Institute*, No. 3, Kiev, Ukraine.
- 572 Santos J.L., Aparicio I., Alonso E., Callejón M., 2005. Simultaneous determination of
573 pharmaceutically active compounds in wastewater samples by solid phase extraction and
574 high-performance liquid chromatography with diode array and fluorescence detectors.
575 *Analitica Chimica Acta* 550, 116–122.
- 576 Schaider L.A., Ackerman J.M., Rudel R.A., 2016. Septic systems as sources of organic
577 wastewater compounds in domestic drinking water wells in a shallow sand and gravel
578 aquifer. *Science of the Total Environment* 547, 470–481.

- 579 Schmidt S.I., Cuthbert M.O., Schwientek M., 2017. Towards an integrated understanding of
580 how micro scale processes shape groundwater ecosystem functions. *Science of the Total*
581 *Environment* 592, 215–227.
- 582 Schmidt S.I., Hahn H.J., Hatton T.J., Humphreys W.F., 2007. Do faunal assemblages reflect
583 the exchange intensity in groundwater zones? *Hydrobiologia* 583, 1–19.
- 584 Shelton J.L., Engle M.A., Buccianti A., Blondes M.S., 2018. The isometric log-ratio (ilr)-ion
585 plot: A proposed alternative to the Piper diagram. *Journal of Geochemical Exploration* 190,
586 130–141.
- 587 Sigman D.M., Casciotti K.L., Andreani M., Barford C., Galanter M., Böhlke J.K., 2001. A
588 bacterial method for the nitrogen isotopic analysis of nitrate in seawater and freshwater.
589 *Analytical Chemistry* 73, 4145–4153.
- 590 Stiff Jr. H. A., 1951. The interpretation of chemical water analysis by means of patterns.
591 *Journal of Petroleum Technology* 3, 15–17.
- 592 Taufiq A., Effendi A.J., Iskandar I., Hosono T., Hutasoit L.M., 2019. Controlling factors and
593 driving mechanisms of nitrate contamination in groundwater system of Bandung Basin,
594 Indonesia, deduced by combined use of stable isotope ratios, CFC age dating, and
595 socioeconomic parameters. *Water Research* 148, 292–305.
- 596 Taylor R.G., Scanlon B., Döll P., Rodell M., van Beek R., Wada Y., Longuevergne L.,
597 Leblanc M., Famiglietti J.S., Edmunds M., Konikow L., Green T.R., Chen J., Taniguchi
598 M., Bierkens M.F.P., MacDonald A., Fan Y., Maxwell R.M., Yechieli Y., Gurdak J.J.,
599 Allen D.M., Shamsudduha M., Hiscock K., Yeh P.J.-F., Holman I., Treidel H., 2012.
600 Ground water and climate change. *Nature Climate Change* 3, 322–329.
- 601 Tipple B.J., Jameel Y., Chau T.H., Mancuso C.J., Bowen G.J., Dufour A., Chesson L.A.,
602 Ehleringer J.R., 2017. Stable hydrogen and oxygen isotopes of tap water reveal structure of

- 603 the San Francisco Bay Area's water system and adjustments during a major drought. *Water*
604 *Research* 119, 212–224.
- 605 Tubau I., Vázquez-Suñé E., Carrera J., Valhondo C., Criollo R., 2017. Quantification of
606 groundwater recharge in urban environments. *Science of the Total Environment* 592, 391–
607 402.
- 608 Unnikrishna P.V., McDonnell J.J., Kendall C., 2002. Isotope variations in a Sierra Nevada
609 snowpack and their relation to meltwater. *Journal of Hydrology* 260 (1–4), 38–57.
- 610 Urresti B., Vadillo I., Jiménez P., Soler A., Sánchez D., Carrasco F., 2015. Application of
611 stable isotopes ($\delta^{34}\text{S-SO}_4$, $\delta^{18}\text{O-SO}_4$, $\delta^{15}\text{N-NO}_3$, $\delta^{18}\text{O-NO}_3$) to determine natural
612 background and contamination sources in the Guadalhorce River Basin (southern Spain).
613 *Science of the Total Environment* 506–507, 46–57.
- 614 Vázquez-Suñé E., Carrera J., Tubau I., Sánchez-Vila X., Soler A., 2010. An approach to
615 identify urban groundwater recharge. *Hydrological Earth System Science* 14(10), 2085–
616 2097.
- 617 Vystavna Y., Diadin D., Yakovlev V., Hejzlar J., Vadillo I., Huneau F., Lehmann M.F., 2017.
618 Nitrate contamination in a shallow urban aquifer in East Ukraine: Evidence from
619 hydrochemical, stable nitrate isotope, and land use analysis. *Environmental Earth Sciences*
620 76 (13), No. 463.
- 621 Vystavna Y., Cherkashyna M., van der Valk M.R., 2018a. Water laws of Georgia, Moldova
622 and Ukraine: current problems and integration with the EU legislation. *Water International*
623 43 (3), 424–435.
- 624 Vystavna Y., Frkova Z., Celle-Jeanton H., Diadin D., Huneau F., Steinmann M., Crini N.,
625 Loup C., 2018b. Priority substances and emerging pollutants in urban rivers in Ukraine:
626 Occurrence, fluxes and loading to transboundary European Union watersheds. *Science of*
627 *the Total Environment* 637–638C, 1358–1362

- 628 Vystavna Y., Huneau F., Diadin D., 2018c. Defining a stable isotope framework for isotope
629 hydrology applications (precipitation, surface and groundwater) for East Ukraine. *Isotopes*
630 in *Environmental and Health Studies* 2(54), 147–167.
- 631 Vystavna Y., Diadin D., Rossi P.M., Gusyev M., Hejzlar J., Mehdizadeh R., Huneau F.,
632 2018d. Quantification of water and sewage leakages from urban infrastructure into a
633 shallow aquifer in East Ukraine. *Environmental Earth Sciences* 77, No. 748.
- 634 WWAP, 2015. United Nations World Water Assessment Programme. The United Nations
635 World Water Development Report 2015: Water for a Sustainable World. Paris, UNESCO.
636 [https://www.un-igrac.org/sites/default/files/resources/files/Groundwater%20overview%20-](https://www.un-igrac.org/sites/default/files/resources/files/Groundwater%20overview%20-%20Making%20the%20invisible%20visible_Print.pdf)
637 [%20Making%20the%20invisible%20visible_Print.pdf](https://www.un-igrac.org/sites/default/files/resources/files/Groundwater%20overview%20-%20Making%20the%20invisible%20visible_Print.pdf)
- 638 Yakovlev V., Vystavna Y., Diadin D., Vergeles Y., 2015. Nitrates in springs and rivers of
639 East Ukraine: distribution, contamination and fluxes. *Applied Geochemistry* 53, 71–78.
- 640 Yin H., Xie M., Zhang L., Huang J., Xu Z., Li H., Jiang R., Wang R., Zeng X., 2019.
641 Identification of sewage markers to indicate sources of contamination: Low cost options
642 for misconnected non-stormwater source tracking in stormwater systems. *Science of the*
643 *Total Environment* 648, 125–134.
- 644
- 645

646 **List of figures**

647 Figure 1. (a) Hydrogeological settings and location of sampling sites. (b) Conceptual diagram
648 of the urban water cycle and sampled components in Kharkiv city, Ukraine.

649 Figure 2. Local meteoric water line (LMWL), annual amount-weighted isotopic composition
650 of precipitation, and position of isotope concentrations in tap water and urban and forest
651 springs in relation to LWML.

652 Figure 3. Ion composition in springs (T1-O6), tap water (TW), and sewage, shown in (a) a
653 Stiff diagram and (b) a Shelton plot.

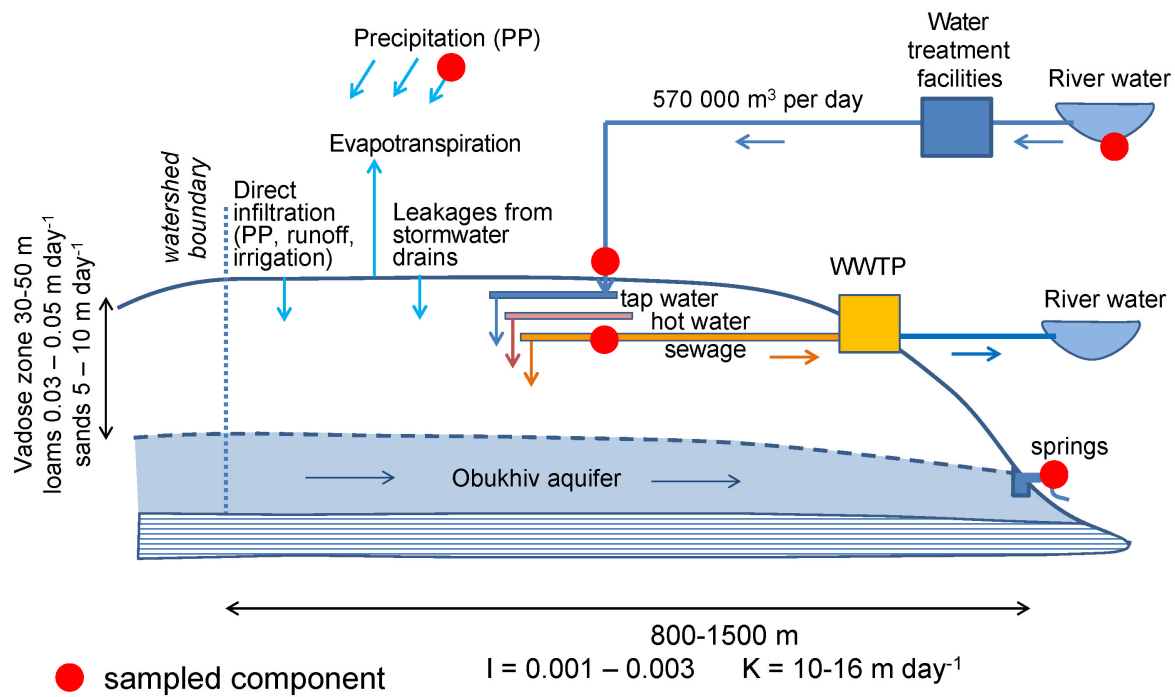
654 Figure 4. Principal component analysis (PCA) plot of relative isotope and geochemical
655 composition of groundwater. Samples are indicated by number (month: 10 = October, 11 =
656 November and so forth) and are connected with arrows according to sampling period.

657 Figure 5. Seasonal variation in discharge, oxygen-18 and nitrate concentrations, and
658 calculated sewage contribution in springs.

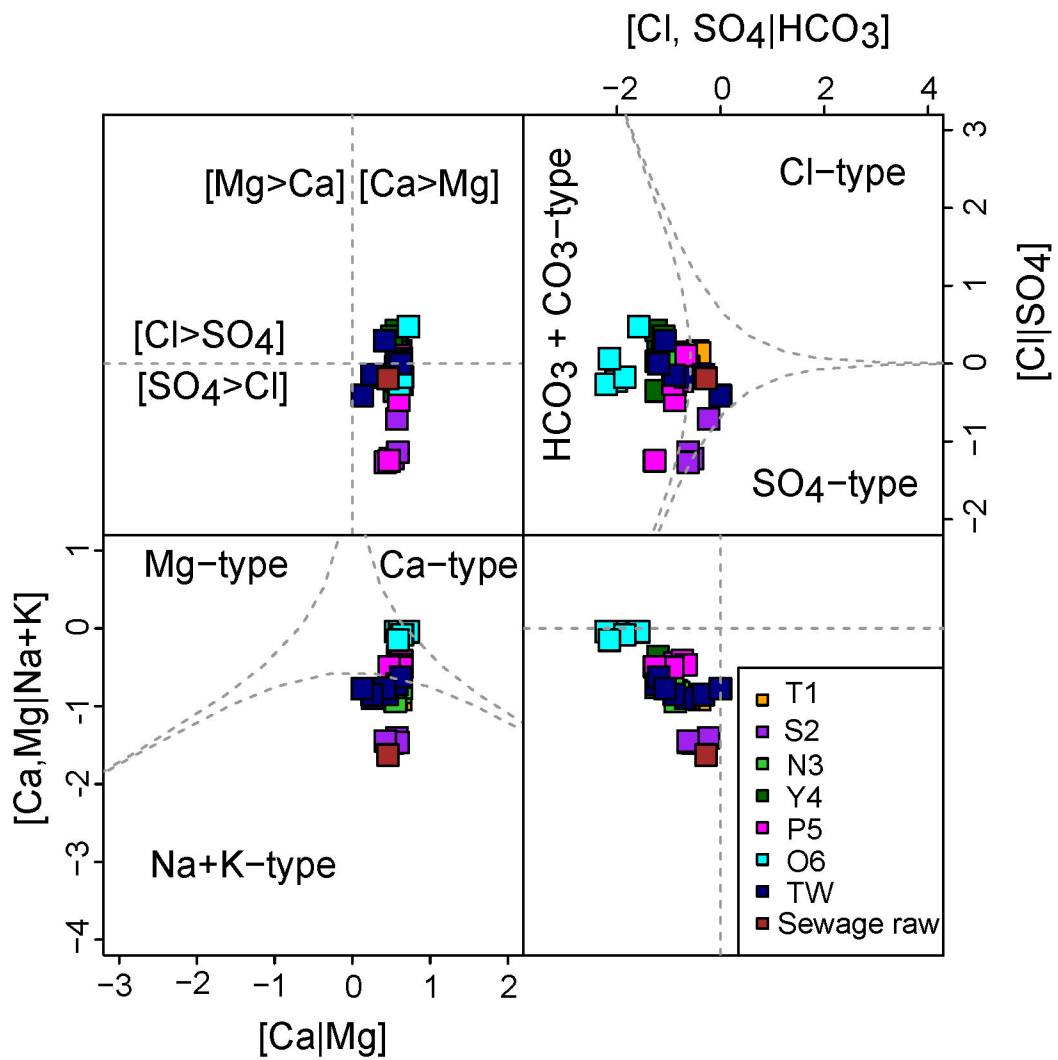
659 Figure 6. Plot of nitrate concentrations and stable isotopes of nitrate in groundwater and tap
660 water. Nitrate source separation according to Kendall (1998).

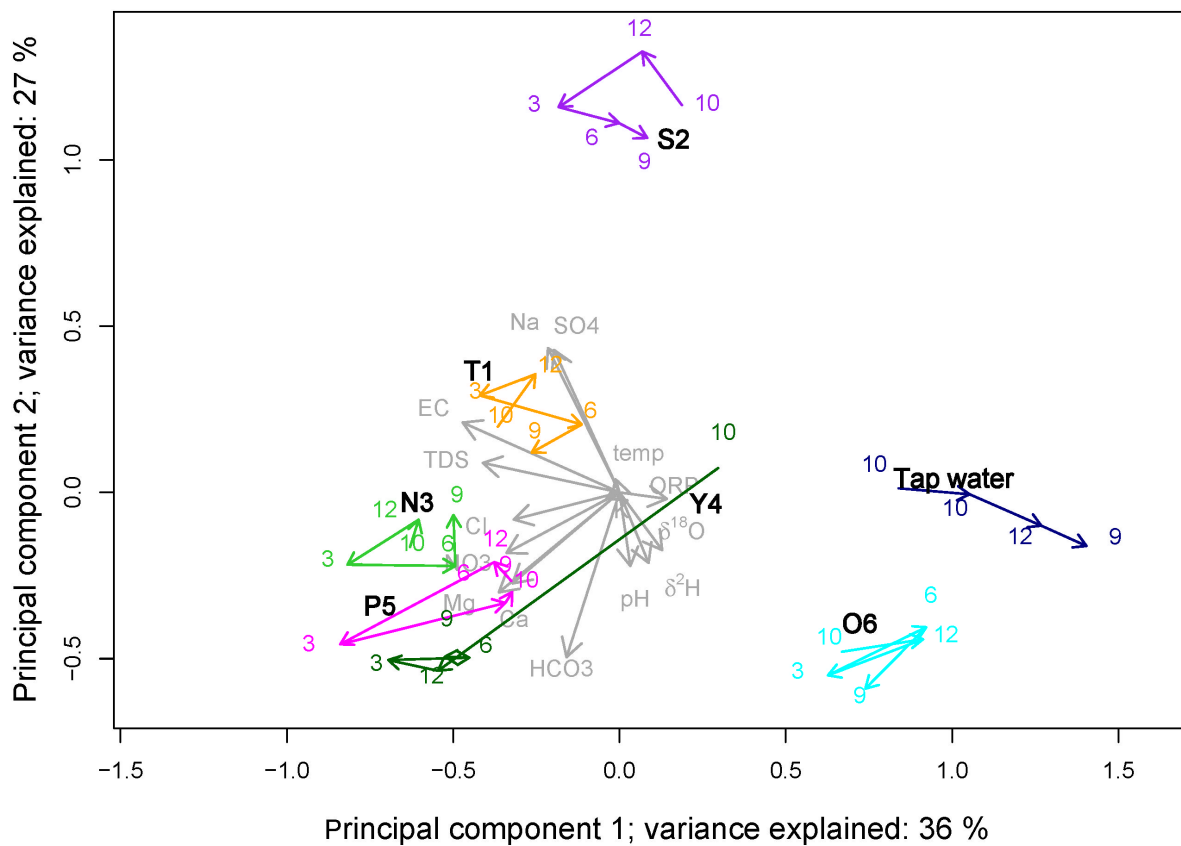
661 Figure 7. Principal component analysis (PCA) plots of isotope composition, geochemical
662 composition, and presence of emerging compounds in groundwater samples.

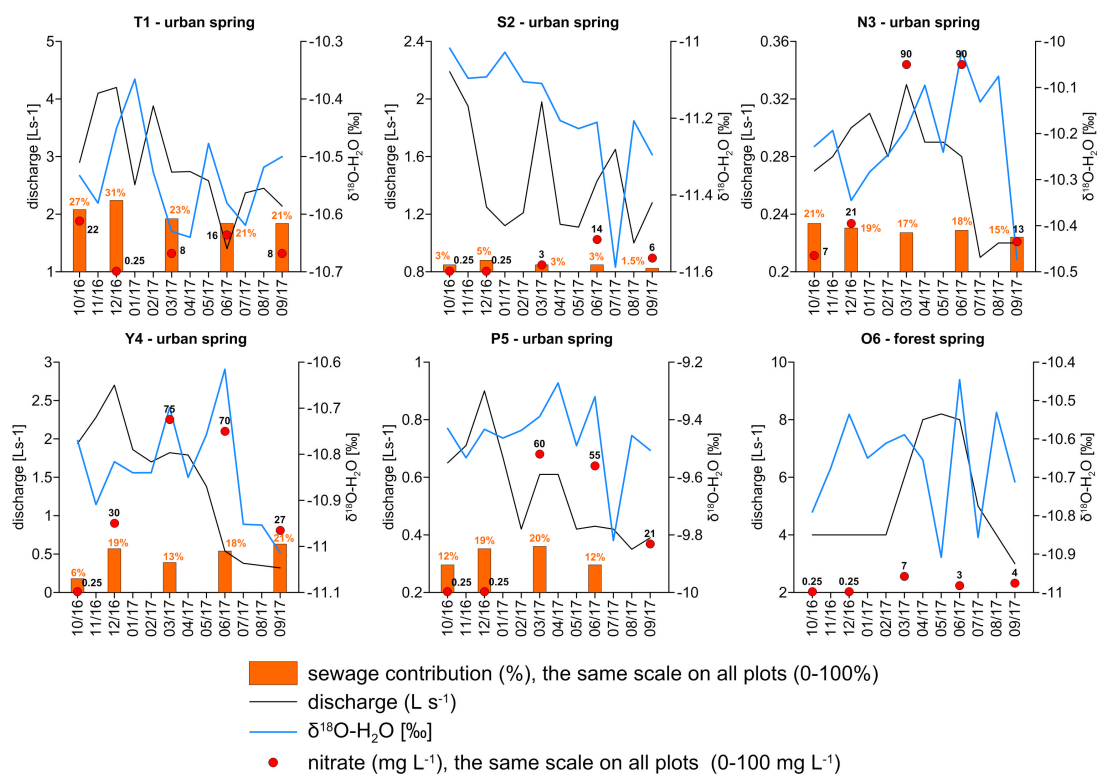
663

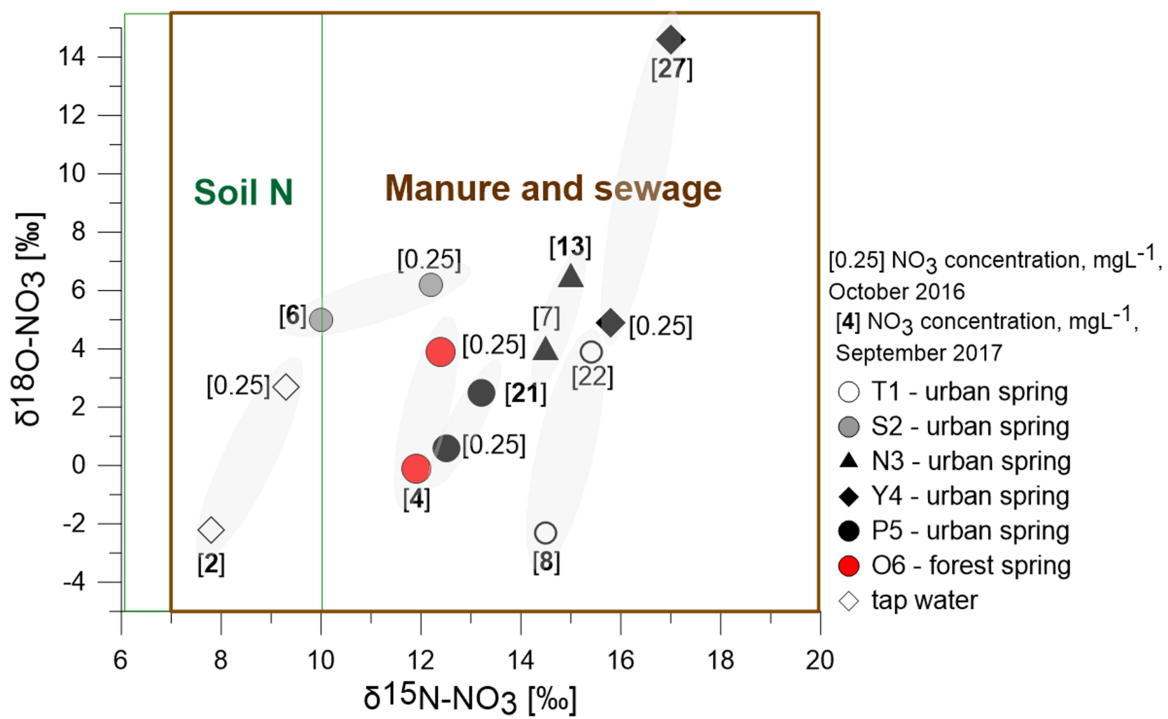


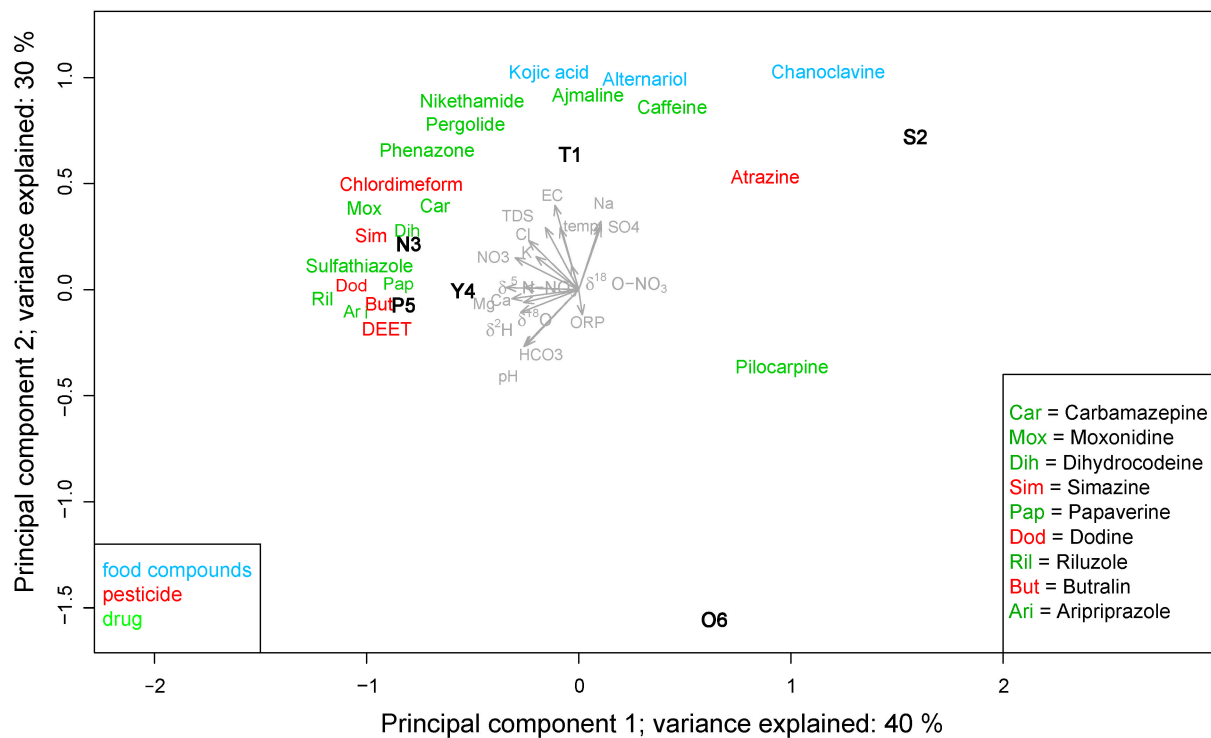
ACCEPTED

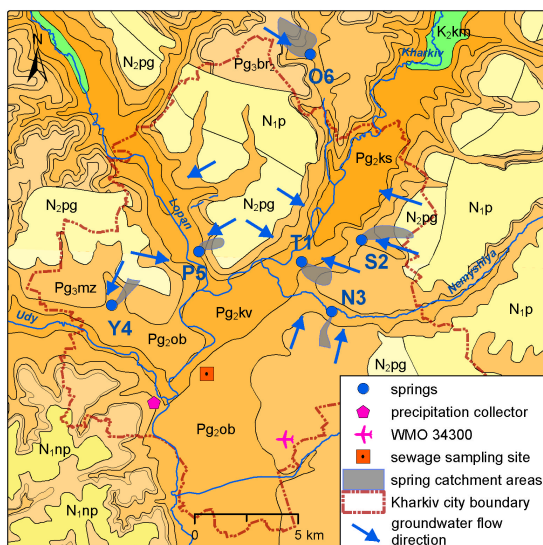










**Paleogene deposits**

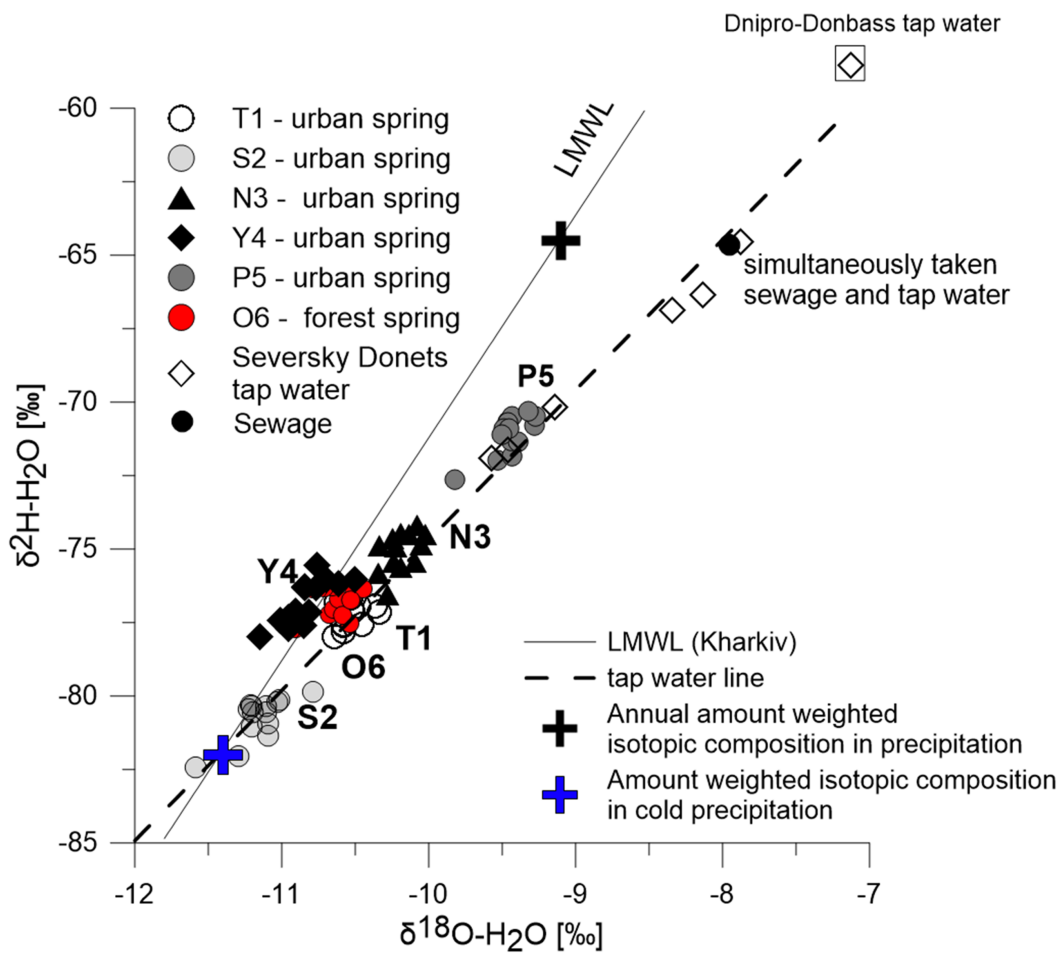
- Pg₃br₂. Sands
- Pg₃br₁. Clays
- Pg₃mz. Sands
- Pg₂ob. Fine-grained sandstones
- Pg₂kv. Clays, marls
- Pg₂ks. Sands
- Pg₂rd. Clays

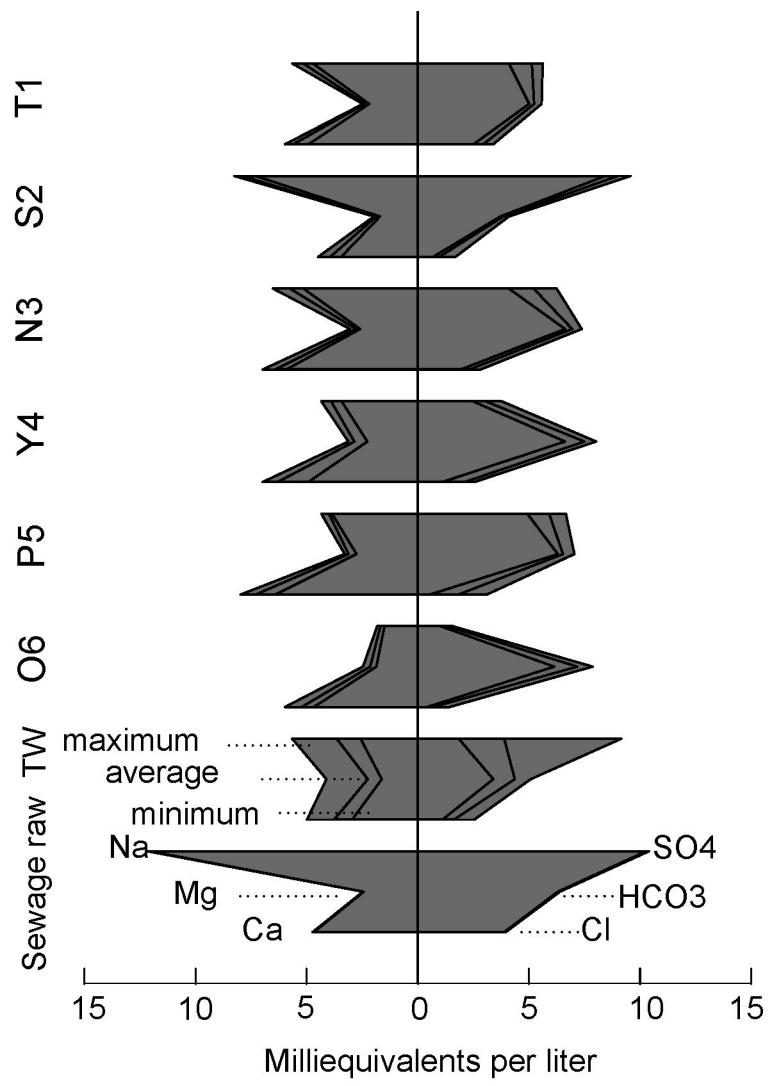
Neogene deposits

- N₂pg. Sands, clays
- N₂cb. Clays
- N₁p. Sands
- N₁sg. Clays
- N₁np. Sands

Cretaceous deposits

- K₂km. Chalk





Highlights:

Urban groundwater quality is highly impacted by sewage inputs

Stable isotopes and emerging contaminants traced sewage leakages to groundwater

Sewage contribution and nitrate content varied seasonally in urban groundwater

Natural $\delta^{18}\text{O}$ extremes in precipitation reflected estimated groundwater transit time

ACCEPTED MANUSCRIPT

Declaration of interests

The authors declare that they have no known competing financial interests or personal relationships that could have appeared to influence the work reported in this paper.

The authors declare the following financial interests/personal relationships which may be considered as potential competing interests:

Declarations of interest: none